7

Circulators

An optical circulator is a generalized isolator having three or more ports. While an isolator causes loss in the isolation direction, a circulator collects the light and directs it to a nonreciprocal output port. Figure 7.1 illustrates several possible circulator configurations. Figure 7.1(a) illustrates the port mapping for a four-port circulator. The ports cyclically map $1 \rightarrow 2 \rightarrow 3 \rightarrow 4 \rightarrow 1$. This is called a strict-sense circulator because every input port has a specific nonreciprocal output port. Construction of a strict-sense circulator with more ports becomes inelegant but ones with three ports can be simple [22]. Figure 7.1(b) illustrates a non-strict-sense circulator having any number of ports greater than two. In this case each input port has a specific nonreciprocal output port except for the last port; the light input to the last port is lost. The ladder diagram reflects the optical path within the component and indicates the disconnect between the first and last ports. Figure 7.1(c) illustrates a three-port non-strict-sense circulator. This circulator has significance in telecommunications applications because return of light from port 3 to port 1 is often not necessary. For instance, the reflected light from a fiber Bragg grating need only be separated from the input light without loss, but as optical links are not typically operated in reverse there is no need for strict-sense behavior.

Other than architecture, most of the considerations for the optical circulator have already been addressed in preceding chapters. As a nonreciprocal device, a circulator has at least one Faraday rotator (FR) in the optical path. The wavelength and temperature performance of FRs was treated in §6.1. In that same section, the transmission and isolation as a function of polarizer alignment was treated. The modern deflection-type circulators use birefringent prism combinations such as the Wollaston and Rochon prisms, detailed in §4.7, along with dual-fiber collimators, detailed in §5.3. Likewise, the differential-group delay due to path-length imbalance was treated in §6.6. Accordingly, all the tools necessary to appreciate and design optical circulators have been earlier developed, allowing the current chapter to focus exclusively on architectures and performance.

Jay N. Damask: Polarization Optics in Telecommunications, SSOS 101, 273–296 (2005)

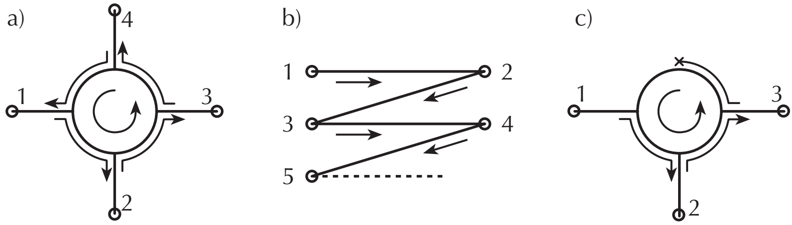

Fig. 7.1. Three types of circulator port connections. a) Strict-sense circulator with four ports. Each input port has a specific nonreciprocal output port. b) Non-strict-sense circulator in ladder topology. Any number of ports greater than two is possible; however, light input to the last port is lost. c) Non-strict-sense three-port circulator. This topology has significant applications in unidirectional telecommunications links and has good economies compared with (a) or (b).

As with isolators, circulators can be polarization dependent or polarization independent. The polarization-dependent circulator is an important starting point because the minimum requirements for circulatory behavior are clear. Polarization-independent circulators are further categorized as displacement-type and deflection-type. Except for the earliest designs, displacement-type circulators use birefringent walkoff crystals to achieve polarization diversity. Deflection-type circulators use birefringent prisms and dual-fiber collimators for the same purpose. The most compact and least expensive circulators use deflection-type designs.

7.1 Polarizing Circulator

Figure 7.2 illustrates a YIG-based polarizing circulator first demonstrated by Shibukawa [32, 33]. This configuration is the minimum necessary to achieve circulatory behavior and should be compared to the polarizing isolator in Fig. 6.1 on page 248. Circulatory behavior exists only for prescribed linear input polarization states. The main issue addressed by Shibukawa was the addition of input and output ports on either side of the FR, as compared to a polarizing isolator, to realize a strict-sense circulator. To create two ports on either side of the FR, Glan-Taylor prisms were used (Fig. 7.2(c)). The Glan-Taylor prisms were used for two reasons. The inventors realized the importance of high polarization contrast yet thin-film polarization beam-splitting cubes were not readily available nor did they exhibit good performance. Moreover, as compared with the Glan-Thompson, Wollaston, and Rochon prisms, the Glan-Taylor prism has a wide deflection angle, e.g. 110° for calcite. This enabled them to build a relatively compact components.

A Glan-Taylor prism is a birefringent prism pair cut so that along the hypotenuse one polarization state, e.g. the extraordinary ray for a positive uniaxial crystal, experiences total-internal reflection at the crystal/air bound-

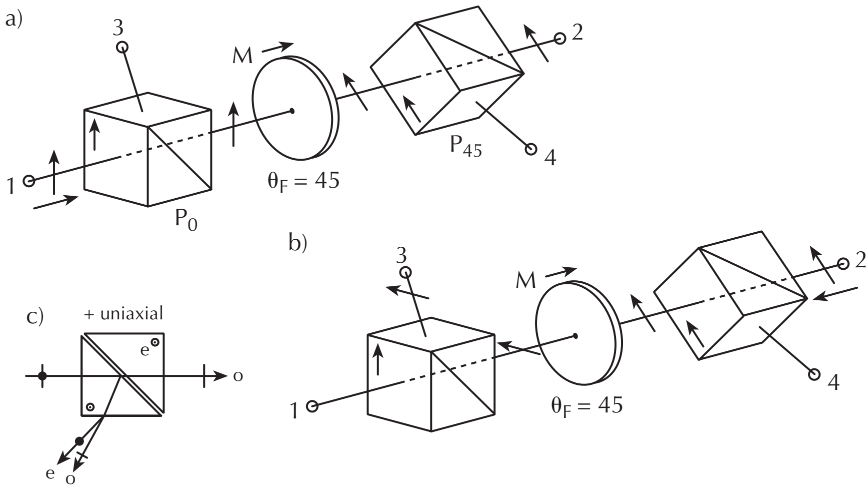

Fig. 7.2. A polarizing circulator in its simplest embodiment. Two polarization-dividing prisms and a Faraday rotator are used. The prisms are rotated by 45° with respect to one another along the longitudinal axis. a) Transmission of $1 \rightarrow 2$ for linear vertical polarization input. Linear horizontal input is deflected by prism $\mathcal{P}_o$. Light after the FR not aligned to prism $\mathcal{P}_{45}$ is output on port 4, reducing path isolation. b) Transmission of $2 \rightarrow 3$ for linear polarization input. Light after the FR not aligned to prism $\mathcal{P}_o$ is output on port 1, reducing path isolation. c) A Glan-Taylor birefringent prism, where e-rays are totally internally reflected and o-rays are partially reflected at the crystal / air interface along the hypotenuse.

ary while the orthogonally polarized ray exits interface. The birefringent prism can be cut at Brewster's angle to maximize the transmission, but such was not the case in the work of Shibukawa. Accordingly, reflected ordinary light co-propagates with the TIR extraordinary light but is refracted at a different angle upon exiting the crystal. It should be noted that in most early demonstrations none of the optical interfaces were anti-reflection coated.

Referring to Fig. 7.2, all that is required for minimal circulatory action is a Faraday rotator with $\theta_F = 45°$, an input polarization splitter, and an output polarization splitter rotated by 45°. To pass from port 1 to port 2, a vertically aligned linear polarization state is input. This state transits the first polarization splitter, is rotated by the FR, and transits the second polarization splitter. In the reverse direction, the same linear polarization state now input to port 2 is again rotated by the FR and is diverted by the first polarization splitter to port 3. Further path tracing shows that this is a strict-sense polarizing circulator.

With high-quality thin-film polarization beam-splitting cubes and high-performance iron garnet materials now available, the polarizing circulator Fig. 7.2 can exhibit good performance other than PDL. However, at the time, losses were incurred through lack of AR coatings, poor extinction ratio of the

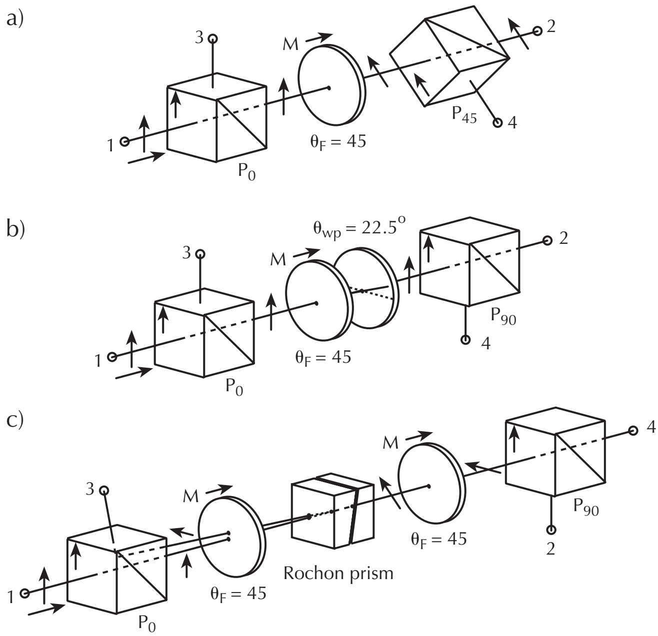

Fig. 7.3. Conceptual development of polarizing circulators. a) Simple polarizing circulator like that of Shibukawa; PBS cubes illustratively replace the Glan-Taylor prisms. The four ports do not lie in a plane. b) Addition of reciprocal element, here a half-wave waveplate, allows all four ports to lie in a plane. The polarization plane can be rotated by 90°. c) A two-stage polarizing circulator. The reciprocal element of (b) is replaced with a second FR and a polarizing beam splitter, such as a Richon prism, located between FR plates. The polarization plane is rotated 90° along the forward path. The polarizing-cube, FR, prism, FR, polarizing-cube sequence forms two-stages of isolation.

prisms, losses in the YIG garnet, and poor fiber coupling. The performance reported at the time is an insertion loss of 2 dB and an isolation variation from 13 dB to 28 dB, depending on port combination. The authors were cognizant of wavelength dependence but made no reports on temperature dependence.

The polarizing circulator leads to a conceptual framework that encompasses essential aspects of any circulator design. The circulator of Shibukawa, or one similar as in Fig. 7.3(a), where the Glan-Taylor prisms are illustratively replaced with polarization beam splitting (PBS) cubes, has four ports that do not lie in a plane. This makes the component form-factor less convenient. To rectify this shortcoming, the FR can be preceded or followed by a reciprocal element such as a half-wave waveplate, having its birefringent axis at ±22.5° with respect to the cube axis, or an optically active crystal that rotates the linear polarization state by 45° (Fig. 7.3(b)). In either case, from the FR looking through the reciprocal plate, the PBS cube that is in view appears rotated by 45°. Optically the cube is rotated but physically it is not, allowing all ports to lie in the same plane.

The reciprocal and nonreciprocal rotators together can rotate the plane of linear polarization by 90°. The 90° rotation is characteristic of most circulators. However, as a general rule a waveplate reduces the bandwidth of a component. Whether such limitation is tolerable or not depends on many factors. Yet a better method is to use two Faraday rotators with an intermediate polarizing beam splitter (Fig. 7.3(c)). Note that other than material dispersion, the second FR has the same wavelength dependence as an equivalent reciprocal rotator. However, the dual FR design accomplishes two goals: the plane of polarization is rotated by 90° in the forward direction and 0° in reverse, and the isolation of the circulator is squared because this is a two-stage circulator. A two-stage circulator is a natural consequence of placing all ports on the same plane.

7.2 Historical Development

Circulator architectures are characterized by rapid development toward an "optimal" design – given available materials, sub-assemblies, and recognized application-specific requirements – and plateaus during which little changed. Very early work in optical circulators circa 1960s derived motivation from radio-frequency circulators which, at the time, required only single-polarization performance [28, 31]. The late 1970s are characterized by the application-specific realization that single-mode optical fiber does not preserve polarization and therefore circulators have to be polarization-independent [17, 29, 36]. Indeed early descriptions claimed a 3 dB loss for a component with infinite polarization-dependent loss (PDL) [17]. Optical circulators thus transformed from polarization-dependent (PD) to polarization-independent (PI) via polarization-diversity schemes. The goal at the time was to achieve high isolation and low loss, which in turn required the development of high-contrast polarization splitters. Specifications of wavelength-dependence and PDL were also recognized at the time, but performance was often poor by today's standards. Temperature dependence was almost never referred to (the exception being [36]) as well as differential-group delay. Lastly, the early PI circulators were strict-sense four-port designs.

Figure 7.4 illustrates the architectural development between 1978 and 1981 from PD circulators to PI circulators. Indeed the submission dates of the articles are so close it is difficult to reconstruct precisely who invented what first. Figure 7.4(a) illustrates the Shibukawa PD circulator detailed in the preceding section. Figures 7.4(b–d) are all PI circulators with an additional important distinction. In all three topologies the four ports lie in the same plane. To do this a reciprocal polarization rotator was added: a half-wave waveplate was used by Matsumoto and Shirasaki, while an optically active

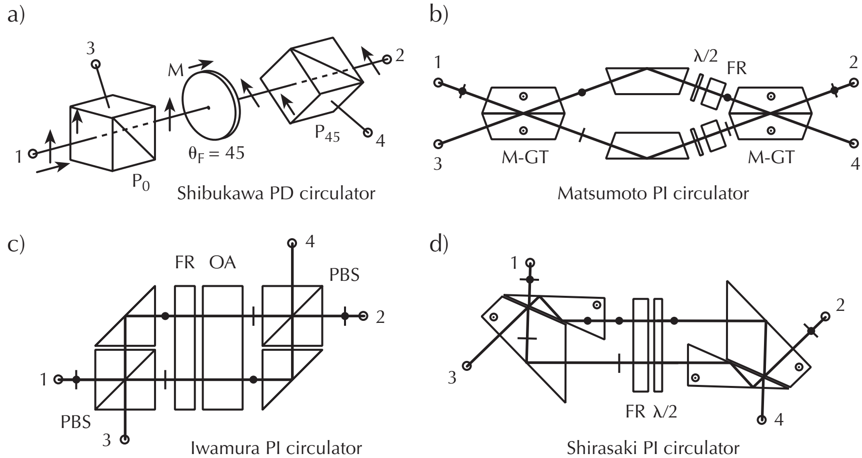

Fig. 7.4. Evolution of early four-port strict-sense circulators. Goals were to provide polarization-independent circulatory behavior with high isolation. a) The polarizing circulator circa 1978. b) First polarization-independent (PI) proposal circa 1979. Modified Glan-Thompson (M-GT) prisms and dual half-wave waveplate plus FR pairs were used. c) Alternative PI proposal circa 1979. Thin-film polarization beam splitters were used, along with optically active quartz for the reciprocal 45°rotation. d) Shirasaki circulator circa 1980 using high-extinction-ratio Shirasaki polarization splitters, an FR and a half-wave waveplate.

(OA) rotator was used by Iwamura. At the time an OA rotator was considered by some as advantageous because of easy alignment [17], although the required crystal length for quartz is 15.8 mm at 1.55 μm [20]. In either case, the addition of the reciprocal rotator reduces the bandwidth of the component.

The Matsumoto PI circulator [28, 29] in Fig. 7.4(b) uses modified Glan-Thompson (M-GT) birefringent prisms to separate the polarization. Similar to the Glan-Taylor prism, the Glan-Thompson prism extracts one polarization component through TIR. The latter prism has the gap between the two prism sections filled with a bonding agent such as epoxy to reduce the angular deflection of the TIR light. Using calcite, Matsumoto reported a 36.4° full-angle deflection. Unlike the Shibukawa PD circulator, the present circulator captures both transmitted and deflected light and directs the two paths through separate half-wave and FR pairs. The waveplate was a true zero-order half-wave waveplate and the FR was YIG with an Sm-Co permanent magnet for saturation. The polarizations output from the rotators are combined by a second Glan-Thompson prism. The reported insertion loss was 3.7 dB.

One principle drawback of the Matsumoto scheme is that the modified Glan-Thompson prisms reflected −12 dB of the non-TIR light in the direction of the TIR light. This made for a very low isolation floor. The other drawback is the duplication of the reciprocal and nonreciprocal rotators.

The Iwamura PI circulator [17] in Fig. 7.4(c) is a far more suitable architecture, but the inventors were limited by the low-quality thin-film polarization beam splitters. The significant improvement is a single reciprocal/nonreciprocal rotator pair through which both optical paths transit. While none of the optical surfaces were anti-reflection coated, the inventors reported an insertion loss of 1.2 – –1.6 dB and an isolation of 16 – –19 dB.

The Shirasaki circulator [22, 36] in Fig. 7.4(d) employs the Shirasaki birefringent prism (cf. §4.7) to act as a high-extinction ratio polarization splitter. Taken as a pair, the rutile prisms exhibited over 40 dB contrast with a loss less than 0.5 dB. Like the Iwamura isolator, the two optical paths run parallel and transit a single rotator pair. The FR was YIG and the half-wave waveplate was a true zero-order quartz plate. It should be noted that the birefringent axis of the waveplate was inclined by 22.5° in the plane perpendicular to the optical path. The resultant circulator had 0.4 – –0.6 dB insertion loss and 25 – –32 dB isolation. Moreover, the inventors characterized their circulator over a 5 – –45° temperature range and demonstrated a 0.3 dB insertion loss shift and ±1 dB isolation variation.

Emkey [7, 9, 10] plays a pivotal role in the development of circulators for two reasons. First, he recognized that birefringent walkoff crystals have a higher extinction ratio than did the polarization-splitting prisms that preceded him. Second, he recognized that for optical communication links a circulator need not be a strict-sense four-port component, but rather a non-strict-sense three-port circulator was satisfactory and certainly more economical. While his component design is awkward and not repeated here, Emkey set the stage for Koga, Fujii, Xie, and others to develop displacement-type circulators in the early 1990s. Displacement-type circulators also incorporated superior iron garnet materials, specifically, the Bi:RIG garnets being developed at the time, and superior single-fiber collimators. A large advance in performance was thus recorded.

The final substantial improvement come about in the late 1990s with the development of the dual-fiber collimator. The dual-fiber collimator simplified and miniaturized the housing size of the lenses. Equally importantly, due to its convenient interaction with Wollaston, Rochon, and Kaifa compound prisms, the use of dual-fiber collimators ushered in a family of deflection-type schemes that substantially reduced the necessary volume of birefringent material, which in turn further reduced the size and cost.

7.3 Displacement Circulators

A displacement-type circulator is one where the polarization components are spatially separated and combined by birefringent crystals cut as walkoff blocks. Birefringent walkoff can yield an extinction ratio between the two polarization components in excess of 50 dB. Such an extinction ratio is better than most commercially available thin-film polarization beam splitting cubes.

Accordingly, the displacement-type circulators developed in the early 1990s exhibited superior performance in comparison with the earlier developed Matsumoto, Iwamura, and Shirasaki circulators.

The series of displacement-type circulators developed by Koga and Matsumoto highlight conceptual developments that have bearing on deflection-type circulators. Their first-reported design was a strict-sense four-port single-stage circulator. The complexity and limited performance of this design was overcome by their second design, which was a non-strict-sense ladder-type two-stage circulator. Even this design, however, was limited in part by the incorporation of reciprocal polarization rotators. These rotators add to the part count and reduce the isolation bandwidth. Their last-reported design was a non-strict sense ladder-type two-stage circulator using only nonreciprocal polarization rotation. This is the most compact and best performing of their devices.

Other inventors have proposed displacement-type circulators as well. In particular, Fujii proposed several designs [11–13] using both walkoff crystals and PBS cubes. Separately, Cheng developed a variety of reflection-based displacement circulators than were more compact that previous architectures [2, 4, 5]. He also addressed issues of low PMD and alignment improvements for manufacturing [3, 6]. More recently, Xie and Huang proposed a compact two-stage design that incorporates thermally expanded-core (TEC) fibers [42]. Use of TEC fibers reduces the necessary beam displacement and in turn the size of the component. TEC fibers will be seen again in the deflection circulators to follow. Finally, Liu *et al.* have proposed a strict-sense four-port two-stage circulator that includes a polarization beam-splitter cube to route the last port back to the first [27].

Figure 7.5 illustrates the first Koga and Matsumoto PI circulator [18, 21]. The core of their circulator is a variation of the Shibukawa PD circulator where the Glan-Taylor prisms are replaced with walkoff blocks (Fig. 7.5(a)). The center reciprocal rotator allows all four ports to lie in the same plane. This PD circulator was embedded between two polarization-conditioning sections that, all together, form a strict-sense circulator (Fig. 7.5(b)). The spot-trace diagrams at the bottom of the figure detail the connection between all port pairs.

As a critique, one can say that the polarization beam splitters to either side of the center FR each require four reciprocal parts. The extinction ratio of the splitters and the insertion loss of the device critically depend on the alignment of these elements. As the circulator is single-stage and the reciprocal parts will be misaligned in a real product, one cannot expect too much from this architecture.

A better design is illustrated in Fig. 7.6. This is a two-stage circulator having fewer components that the first design [18, 20, 21]. The simpler architecture was achieved by switching to a ladder-type device from a strict-sense device. Reciprocal rotators are still included, but the two-stage design helps with the isolation. As with the first device, all paths into and out of the cir-

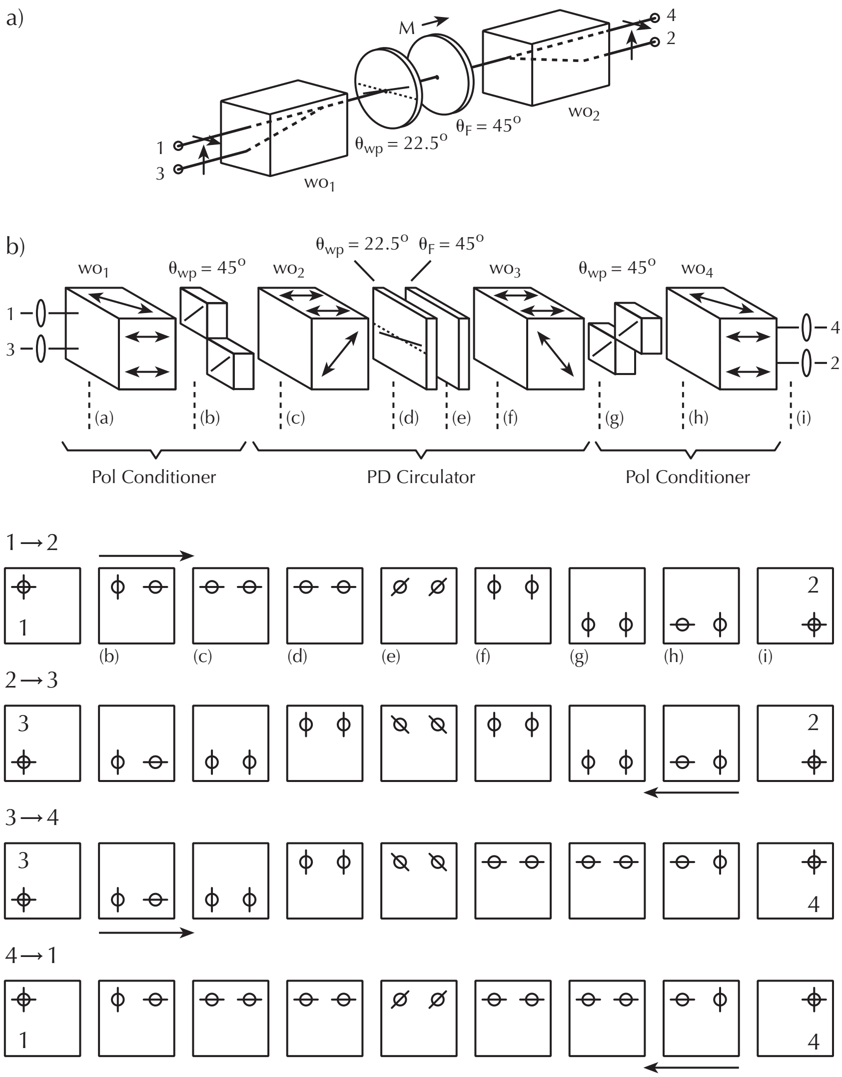

Fig. 7.5. Koga and Matsumoto strict-sense single-stage displacement-type circulator [18, 21], altered by the author to include half-wave waveplates rather than optically active plates and to simplify the quarter-size elements. a) A variation of the Shibukawa PD circulator, where walkoff blocks substitute for Glan-Taylor prisms and a half-wave waveplate allows all four ports to lie in the same plane. b) The PI circulator with embedded PD circulator. The polarization-conditioning stages generate the strict-sense PI circulatory behavior. All paths into and out of the circulator run parallel, and four separate collimators couple the light to and from fiber. At the bottom, spot-trace diagrams detail the connection between port pairs.

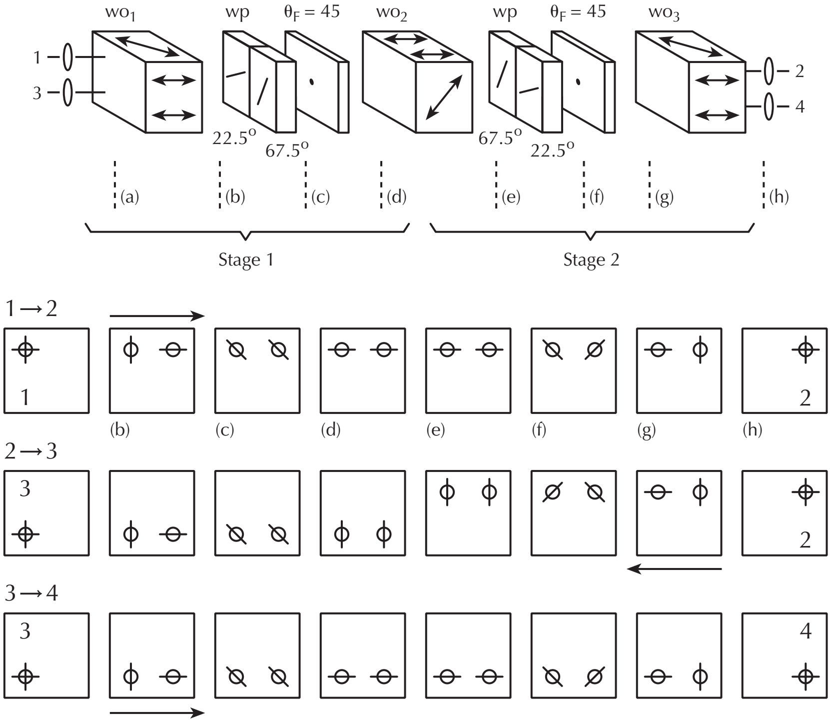

Fig. 7.6. Koga and Matsumoto ladder-type two-stage displacement circulator [18, 20, 21], altered by the author to include half-wave waveplates rather than optically active plates. The center walkoff block is the polarizing element between the first and second Faraday rotators, resulting in a two-stage circulator. All paths into and out of the circulator run parallel, and four separate collimators couple light to and from fiber. At the bottom, spot-trace diagrams detail the connection between port pairs. The connection 4 → 1 is not available.

culator are parallel, and separate collimating lenses were used to couple to and from the fiber. Given a minimum spacing of adjacent collimators based on the form factor, the displacement crystals must be long enough to couple to either lens. Koga and Matsumoto somewhat overcame this limitation by using turning prisms to deflect the light from a small core to a more widely spaced lens pair. However, use of turning prisms in production is not often attractive. Nonetheless, the inventors reported an insertion loss of < 1.5 dB, a PDL of 0.25 dB, and isolation at room temperature and center wavelength of over 67 dB. They reported a 70 nm wavelength range centered at 1550 nm where the isolation was at least 60 dB.

The final architecture in this series eliminates the reciprocal rotators all together [19], developed by Koga. The stated purposed by the inventor was to reduce the component length by removing the optically active rotators.

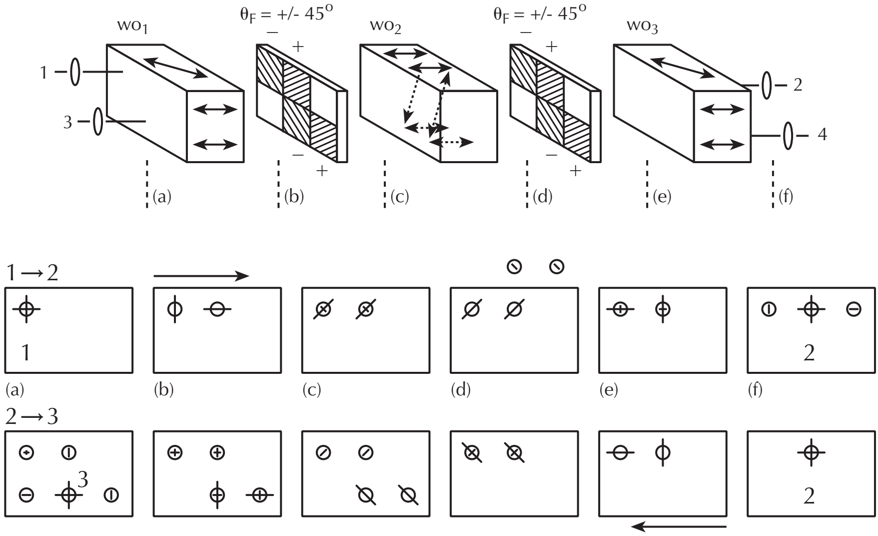

Fig. 7.7. A ladder-type two-stage displacement circulator with no reciprocal rotators, proposed by Koga [19]. Tiled FR elements are located between walkoff blocks. The center walkoff block walks the extraordinary rays along a 45° line in the plane perpendicular to the long component axis. All paths into and out of the circulator run parallel, and four separate collimators couple light to and from fiber. At the bottom, spot-trace diagrams detail the connection between port pairs as well as the error paths.

However, substantial length reduction could well have been achieved through substitution of half-wave waveplates. Nonetheless, the bandwidth of the resultant component is increased by the removal of the reciprocal rotators.

The quartz-free two-stage ladder-type circulator demonstrated by Koga is illustrated in Fig. 7.7. Here a checkerboard of FR elements is used to intersect the internal optical paths in the appropriate way to create a PI circulator. The center walkoff block is also changed to impart walkoff along a 45° direction in the plane perpendicular to the light path. Since the spacing in the FR checkerboard was small, only one external magnet could be used. To achieve both clockwise and counterclockwise polarization rotation the inventor used two different Faraday materials, YIG and a Bi:RIG derivative. The drawback was that the YIG garnet was 2.1 mm thick and the Bi:RIG garnet was 0.48 mm thick. This leads to a relatively high PDL (1.1 dB) and a differential group delay of 21 ps (although no more than about 8 ps can be accounted for via index and path-length difference alone). Also, while not reported, the temperature coefficients of these two materials differ, reducing the isolation over a normal operating range. Nonetheless, it was reported that the insertion loss was below 1.75 dB and the isolation better than 65 dB.

It should be noted that the YIG and Bi:RIG garnets can be replaced today with matched latching garnets. The ±45° rotations are realized by reversing the orientation of one part with respect to the other part. Also, the permanent magnet is removed. Using latching garnets, one expects the PDL, temperature dependence, and differential-group delay to improve substantially.

As a final note, like the earlier displacement circulators, the input and output ports are parallel to one another and individual collimators couple the light to fiber. The component size cannot be reduced beyond the displacement necessary for light to couple to either of two collimators on the same side of the component. As a consequence, there is a minimum volume of required crystal material which sets a floor on the price. These limitations are overcome by deflection circulators.

7.4 Deflection Circulators

The size of a circulator can be reduced by using a dual-fiber collimator. A dual-fiber collimator uses a single lens to collimate or focus the light from two closely-spaced fibers threaded through the same ferrule. As derived in §5.3, the consequence of using a single lens for two fibers is an angular divergence between collimated light paths. A typical full-angle divergence is 3°, although this varies by product.

Combination of dual-fiber collimators (DFC) with deflection prisms is natural. The simplest example of coupling a single-fiber collimator to a dual-fiber collimator is the polarization-beam splitter. Figure 7.8 illustrates four polarization-beam splitters, all of which use a birefringent prism for deflection. Figure 7.8(a) uses a Wollaston prism to convert parallel paths to paths that match the angular aperture of the DFC, and uses a walkoff crystal to laterally translate the beams into position [14]. Figure 7.8(b) combines the first two crystals into one, and when combined with a second prism, as shown, the combination is called the Kaifa prism (cf. §4.7.2). As with the first example, one beam is displaced before the two beams are deflected into the angular aperture of the DFC. Figure 7.8(c) achieves displacement by concatenating two Wollaston prisms with a "complete gap" in between [16]. The second Wollaston prism imparts stronger deflection that the first and orients the light into the angular aperture of the DFC. These three polarization-beam splitters all require translation of one or both beams because there is a presumption that large optical elements will be inserted between the collimators. However, very small-size designs may place the effective deflection plane of a prism right at the crossing point of the DFC [15, 25]. Specially designed DFCs can have crossing distances of ~ 2.4 mm. Figure 7.8(d) illustrates a Wollaston prism located as described to form a compact polarization-beam splitter.

As a critique of the first three designs, the third polarization-beam splitter uses less crystal volume than the first two. The deflection from the first prism makes the two beams diverge, creating displacement without the need for

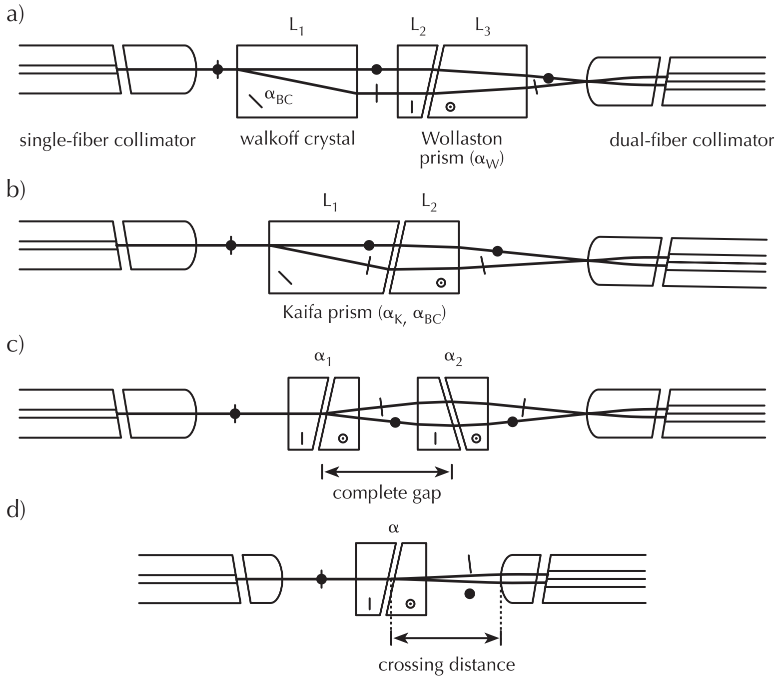

Fig. 7.8. Four polarization-beam splitters using deflection from compound birefringent prisms to match the angular aperture of an output dual-fiber collimator. a) Combined walkoff crystal and Wollaston prism. The prism imparts deflection into the angular aperture of the DFC, while the walkoff crystal provides the necessary translation. b) The Kaifa compound prism combines walkoff and deflection in one compound prism. c) A pair of Wollaston prisms with an intermediate complete gap. The second prism imparts more deflection than the first. The complete gap is adjusted to fine-tune the spatial translation for optimal coupling. d) Single Wollaston prism placed at the crossing point of a DFC. Such a system typically has a small gap between lenses.

crystal. Also, the complete gap is a convenient alignment degree-of-freedom unavailable in the first two designs. The forth splitter uses the least crystal volume of all but requires that all necessary parts fit between the ferrule and the crossing point.

Based on this primer, five significant circulator architectures are detailed in the following. These circulators are all deflection-type, non-strict-sense three or four port components that were independently developed between 1997 and 1999. The first two circulators are the Kaifa designs, invented by Li, Au-Yeung, Guo, and Wang. The third and last circulators are New Focus designs invented by Xie and Huang. The fourth circulator is a Fujitsu-Avanex design invented by Shirasaki and Cao. These designs highlight the aforementioned techniques to integrate dual-fiber collimators into two-stage circulators.

Kaifa Circulators

Figure 7.9 illustrates a Kaifa non-strict-sense two-stage three-port circulator that uses a deflection scheme [23, 24]. The chain of optical elements is shown is Fig. 7.9(a). Polarization diversity is carried out in the vertical plane via walkoff crystals wo_1 and wo_3, while deflection happens in the horizontal plane via the Wollaston prism and walkoff crystal wo_2. The separation of polarization diversity and deflection into orthogonal planes is important because fine placement adjustments can be made independently of one another. The circulator is two-stage because each FR is located between a walkoff-crystal polarizer or compound prism polarizer. The nonreciprocal FR plates are each preceded by a reciprocal half-wave waveplate pair. The pair is split along the horizontal and oriented so that, at the center wavelength of the waveplates, one plate rotates the polarization state by $+45°$ while the other imparts a rotation of $-45°$. Figures 7.9(b,c) show the spot-trace diagrams, and the top- and side-view of the component for connections $1 \rightarrow 2$ and $2 \rightarrow 3$.

As a critique, the reciprocal elements add to the part count, may be difficult to precisely align, and reduce the isolation bandwidth. Moreover, the second walkoff-block is an unnecessary addition to the part count.

These two problems are remedied in the second Kaifa design, shown in Fig. 7.10 [1]. Like the first, this circulator is a non-strict-sense two-stage three-port circulator, but here the Kaifa compound prism is incorporated to impart displacement and deflection. Moreover, the reciprocal half-wave waveplates are eliminated. To accommodate the elimination, the Faraday rotator plates are each split in two, the upper having a rotary direction clockwise and the lower having an opposite rotary direction; and the first and third walkoff crystals are re-cut to displace light along a 45° angle (rather than vertical) in the plane perpendicular to the longitudinal axis of the component. This change in crystal cut rotates by 45° the output polarizations of the displaced and straight-through beams. The polarization states impingent on the Kaifa prism in either direction remain that same as those in Fig. 7.9.

The result of the re-cut of the first and third walkoff blocks is a coupling of the horizontal and vertical axes, which makes alignment more difficult. However, the component has three fewer parts and no reciprocal rotators.

A First Xie-Huang Circulator

A first Xie-Huang deflection-type circulator is illustrated in Fig. 7.11 [40, 41, 43]. This circulator is in the same spirit as the Kaifa circulators, and is a non-strict-sense two-stage three-port design. While the first Kaifa circulator uses waveplates and the second circulator eliminates them but couples the horizontal and vertical axes, the present Xie-Huang circulator combines the best features of the two. At the core of the Xie-Huang circulator is a pair of Wollaston prisms separated by a complete gap. As with the aforementioned polarization-beam splitters, one prism deflects more strongly than the other.

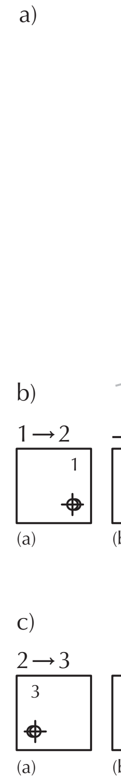

Fig

a)

b)

$1 \rightarrow 2$

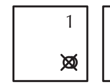

(a)

c)

$2 \rightarrow 3$

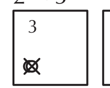

(a)

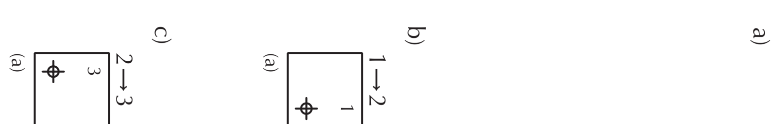

Fig. 7.1

The combination of the weaker prism and the complete gap together generate the displacement embodied by the Kaifa designs. However, since the orientation of the birefringent axes in the Wollaston prisms is arbitrary, the Xie-Huang design uses a modified Wollaston prism pair with birefringent axis orientations of $\pm 45°$. These axes are directly aligned to the polarization states resolved by the walkoff crystals and the Faraday rotator pairs. Accordingly, the polarization diversity generated by walkoff crystals wo_1 and wo_2 may be in the plane perpendicular to the deflection of the Wollaston prism pair. Moreover, the Wollaston prism pair allows for simultaneous elimination of differential-group delay and balancing of diffraction along the two paths. These properties lead to low PMD and low PDL, respectively.

The complete gap is an ingenious feature that allows fine-tuned alignment between collimators. The convergence angle may be just a few degrees. For instance, a $3°$ convergence angle gives a $20 : 1$ ratio between longitudinal adjustment and lateral displacement.

The inventors use latching iron garnet Faraday rotators to eliminate the permanent magnets and to allow the same material to be used for both rotary directions in the pair. This is an important innovation that reduces size and balances paths, and is possible because the two-stage isolation accommodates the increased temperature sensitivity of the latching garnet.

Shirasaki-Cao Circulator

To make a circulator smaller yet, the displacement for the polarization diversity must be reduced. The displacement, of course, must be sufficient to separate light into two distinct beams. Shirasaki and Cao impart displacement at the ferrule and before the lens, where the beam waist is on the order of 10 μm (separately noted in [26]). The displacement crystal need only be ~ 100 μm thick, a factor of $25\times$ reduction from a typical crystal length where the walkoff follows the lens. With the removal of walkoff crystals from the optical path between the lens pair, there is room to place the deflection prism at the crossing point of the dual-fiber collimator. Architectures of this type are the most compact of all circulator.

Figure 7.12 illustrates the Shirasaki-Cao non-strict-sense two-stage four-port circulator [35], an improvement on an earlier design by Shirasaki [34]. As a four-port scheme, dual-fiber collimators are located on either end of the component. While any deflection prism may be used, the illustration shows a Rochon prism. As shown in Fig. 7.12(a), the walkoff and deflection directions are orthogonal, which decouples the adjustment of polarization diversity from isolation. Also note that in contrast to the preceding deflection-type circulators the present design uses a cross-over design in the plane of polarization-diversity. The lens axis is located between the axes of the walkoff light and straight-through light so as to deflect both paths equally.

In this architecture, a walkoff crystal and half-wave waveplate are located between the ferrule and lens (Fig. 7.12(a)). Accordingly, the polarizations on a)

b)

c)

the two paths at the lens are nominally the same. After the lens, the polarization state is rotated by 90° by transit of the first and second Faraday rotators. The deflecting prism located between the two FRs is cut so that the birefringent axes are at ±45°. Using a Rochon prism, one polarization state (i.e. +45°) is transmitted straight through while the orthogonal state is deflected. As shown by the ray-trace diagrams in Fig. 7.12(b,c), the component can be designed so that no deflection makes the connections $1 \rightarrow 2$ and $3 \rightarrow 4$, while deflection makes the connection $2 \rightarrow 3$. Light input to port 4 is deflected and lost toward point P. As discussed by the inventors, the diffraction of the u-path is less than the v-path because the former path transits the two waveplates. Moreover, the differential diffraction occurs in the high N.A. region between ferrule and lens. In principle this leads to either higher insertion loss or higher PDL. If a particular design cannot be made satisfactorily, a glass plate can be inserted beside the waveplate to balance the diffraction.

As a critique, the presence of the waveplates limits the bandwidth of the device. Moreover, the Rochon prism should be as thin as possible to minimize the imparted differential-group delay. Otherwise, the Shirasaki-Cao design is very compact and overall rather simple to make.

A Second Xie-Huang Circulator

Many variations are possible with the Shirasaki-Cao architecture, some of which depend on the particular technologies that are employed. An independently invented Xie-Huang circulator that falls into this class is illustrated in Fig. 7.13 [44]. Here the Faraday rotator plates are brought between the ferrule and lens. The plates are split in two along a horizontal line and the plates impart opposite rotations. This allows the removal of the half-wave waveplates present in the former scheme. This step is technically difficult for the following reasons. The FRs must be latching garnets to enable opposite rotation with the same material. A latching garnet thickness for 1.55 μm applications is ~ 500 μm thick instead of ~ 350 μm thick for non-latching Bi:RIG garnets. The latching garnet thickness is to be compared to the half-wave waveplate thickness of 92 μm.

The five-fold thickness increase, especially between ferrule and lens, requires more displacement and a larger lens. Alternatively, the inventors use TEC fiber to reduce the numerical aperture of the light emergent from the ferrule. It is in this way the split-FR highly compact design can be realized.

Figure 7.13(a) illustrates their non-strict-sense two-stage three-port circulator. Since only three ports are used (and accordingly only one DFC), the deflecting prism is naturally a Wollaston prism. When viewed from port 2, one polarization is deflected toward port 1 and the other towards port 3. The ray-trace diagrams in Fig. 7.13(b,c) show the $1 \rightarrow 2$ and $2 \rightarrow 3$ connections. Light input to port 3 is deflected to the region above port 2 and is lost. Since this circulator is diffraction, path-length, and temperature balanced between

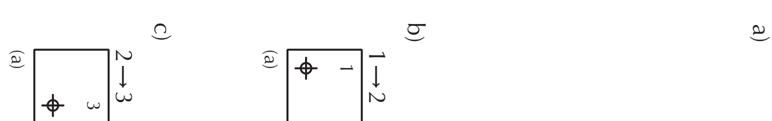
a)
b)
c)
1→2
2→3
(a)
(a)
1
3

Table 7.1. Two-Stage Deflection-Type Circulator Performance

Specification[a]	**Nominal**	**Units**
Center wavelength	1550	nm
Bandwidth	50	nm
Isolation (λ_c, 23°C, all SOP)	50	dB
Isolation ($\lambda_c \pm 25$ nm, 0-65°C, all SOP)	40	dB
Insertion Loss (λ_c, 23°C, all SOP)	0.5	dB
Insertion Loss ($\lambda_c \pm 25$ nm, 0-70°C, all SOP)	0.7	dB
PMD	0.05	ps
PDL	< 0.15	dB
Return loss	50	dB
Maximum crosstalk	-50	dB
Power handling	500	mW
Operating temperature	0–65	°C

[a]Specification values reported by New Focus [30].

the two paths, one can expect very good performance. Table 7.1 lists the specifications for a high-performance compact circulator such as this one.

7.5 Summary

Circulator architectures have experienced periods of rapid and competitive development followed by relatively stable design concepts. The two driving factors behind periods of development are the advent of new materials and sub-assemblies, such as iron garnets and dual-fiber collimators, as well as application-specific demands, such as compact form factor and low polarization-dependent loss. This chapter has selected from the broader patent and technical literature those circulators that highlight the conceptual evolution. Within the framework developed here other circulators may be categorized and then one can make a prediction on its relative performance.

At the time of this writing initiatives to create new functionality are being developed. The bi-isolator [39] and the bi-circulator [8, 37, 38] are two leading examples. Both components are designed to work on a uniformly spaced wavelength-division multiplexed grid in order to facilitate bi-directional communication. Consider the separation of DWDM wavelengths into even and odd channels, and run the even channels "east" and the odd channels "west." On even channels, the bi-isolator prevents light from travelling west; on odd channels the bi-isolator prevents light from travelling east. The bi-circulator operates as a similar principle in that the component circulates "clockwise" for even channels and "counterclockwise" for odd channels. The bi-circulator can act as a gateway between unidirectional and bidirectional communication systems. The element common to both the bi-isolator and bi-circulator is an interleaving filter. The filter designs are discussed in the references.

References

1. V. Au-Yeung, Q.-D. Gao, and X. L. Wang, "Optical circulator," U.S. Patent 6,331,912, Dec. 18, 2001.
2. Y. Cheng, "Reflective optical non-reciprocal devices," U.S. Patent 5,471,340, Nov. 28, 1995.
3. ——, "Optical circulator," U.S. Patent 5,574,596, Nov. 12, 1996.
4. ——, "Optical circulator," U.S. Patent 5,878,176, Mar. 2, 1999.
5. ——, "Optical circulator," U.S. Patent 5,930,422, June 27, 1999.
6. ——, "Optical circulator," U.S. Patent 5,991,076, Nov. 23, 1999.
7. J. S. V. Delden, "Optical circulator having a simplified construction," U.S. Patent 5,212,586, May 18, 1993.
8. T. Ducellier, K. Tai, K.-W. Chang, J. Chen, and Y. Cheng, "Bi-directional circulator," U.S. Patent 2002/00 224 730, Feb. 28, 2002.
9. W. L. Emkey, "A polarization-independent optical circulator for 1.3 microns," *Journal of Lightwave Technology*, vol. LT-1, no. 3, pp. 466–469, Sept. 1983.
10. ——, "Optical circulator," U.S. Patent 4,464,022, Aug. 7, 1984.
11. Y. Fujii, "High-isolation polarization-insensitive optical circulator," *Journal of Lightwave Technology*, vol. 9, no. 10, pp. 1238–1243, Oct. 1991.
12. ——, "High-isolation polarization-insensitive optical circulator coupled with single-mode fiber," *Journal of Lightwave Technology*, vol. 9, no. 4, pp. 456–460, Apr. 1991.
13. ——, "High-isolation polarization-insensitive quasi-optical circulator," *Journal of Lightwave Technology*, vol. 10, no. 9, pp. 1226–1229, Sept. 1992.
14. Y. Huang and P. Xie, "Optical polarization beam combiner/splitter," U.S. Patent 6,331,913, Dec. 18, 2001.
15. ——, "Optical polarization beam combiner/splitter," U.S. Patent 6,282,025, Aug. 28, 2001.
16. ——, "Optical polarization beam combiner/splitter," U.S. Patent 6,373,631, Apr. 16, 2002.
17. H. Iwamura, H. Iwasaki, K. Kubodera, Y. Torii, and J. Noda, "Compact optical circulator for near-infrared region," *Electronics Letters*, vol. 15, no. 25, pp. 830–831, Dec. 1979.
18. M. Koga, "Optical circulator," U.S. Patent 5,204,771, Apr. 20, 1993.
19. ——, "Compact quatzless optical quasi-circulator," *Electronics Letters*, vol. 30, no. 17, pp. 1438–1440, Aug. 1994.
20. M. Koga and T. Matsumoto, "Polarisation-insensitive high-isolation nonreciprocal device for optical circulator application," *Electronics Letters*, vol. 27, no. 11, pp. 903–905, May 1991.

21. ——, “High-isolation polarization-insensitive optical circulator for advanced optical communication systems,” *Journal of Lightwave Technology*, vol. 10, no. 9, pp. 1210–1217, Sept. 1992.
22. H. Kuwahara, “Optical circulator,” U.S. Patent 4,650,289, Mar. 17, 1987.
23. W.-Z. Li, V. Au-Yeung, and Q.-D. Gao, “Optical circulator,” U.S. Patent 5,909,310, June 1, 1999.
24. ——, “Optical circulator,” U.S. Patent 5,930,039, July 27, 1999.
25. W. Z. Li and Y. Yang, “Method and system for splitting or combining optical signal,” U.S. Patent 6,353,691, Mar. 5, 2002.
26. W. Z. Li, Y. Yang, F. Liu, and W. Luo, “Polarization splitter and combiner and optical devices using the same,” U.S. Patent 6,493,140, Dec. 10, 2002.
27. Z. Liu, M. S. Wang, and J. Xu, “Loop optical circulator,” U.S. Patent 2003/0 007 244 A1, Jan. 9, 2003.
28. T. Matsumoto, “Optical circulator,” U.S. Patent 4,272,159, June 9, 1981.
29. T. Matsumoto and K. Sato, “Polarization-independent optical circulator: An experiment,” *Applied Optics*, vol. 19, no. 1, pp. 108–112, Jan. 1980.
30. “New focus optical circulators (c-band),” New Focus Corporation, San Jose, California, 2003. [Online]. Available: http://www.newfocus.com/Online_Catalog/literature/Cband.pdf
31. W. B. Ribbens, “An optical circulator,” *Applied Optics*, vol. 4, pp. 1037–1038, 1965.
32. A. Shibukawa and M. Kobayashi, “Compact optical circulator for near-infrared region,” *Electronics Letters*, vol. 14, no. 25, pp. 816–817, Dec. 1978.
33. ——, “Compact optical circulator for optical fiber transmission,” *Applied Optics*, vol. 18, no. 21, pp. 3700–3703, Nov. 1979.
34. M. Shirasaki, “Optical device,” U.S. Patent 5,982,539, Nov. 9, 1999.
35. M. Shirasaki and S. Cao, “Optical circulator or switch having a birefringent wedge positioned between faraday rotators,” U.S. Patent 6,226,115, May 1, 2001.
36. M. Shirasaki, H. Kuwahara, and T. Obokata, “Compact polarization-independent optical circulator,” *Applied Optics*, vol. 20, no. 15, pp. 2683–2687, Aug. 1981.
37. K. Tai, Q. Guo, K. W. Chang, J. Chen, and M. Xu, “4-port interleavers and fully circulating bi-directional circulators,” in *Tech. Dig., Optical Fiber Communications Conference (OFC’01)*, Anaheim, CA, Mar. 2001, paper MK5.
38. K. Tai, K.-W. Chang, J. Chen, T. Ducellier, and Y. Cheng, “Wavelength-interleaving bidirectional circulators,” *IEEE Photonics Technology Letters*, vol. 13, no. 4, pp. 320–322, 2001.
39. ——, “Bi-directional isolator,” U.S. Patent 6,587,266, July 1, 2003.
40. P. Xie and Y. Huang, “Compact polarization insensitive circulators with simplifed structure and low polarization mode dispersion,” U.S. Patent 6,049,426, Apr. 11, 2000.
41. ——, “Compact polarization insensitive circulators with simplifed structure and low polarization mode dispersion,” U.S. Patent 6,052,228, Apr. 18, 2000.
42. ——, “Compact polarization insensitive circulators with simplifed structure and low polarization mode dispersion,” U.S. Patent 6,212,008, Apr. 3, 2001.
43. ——, “Compact polarization insensitive circulators with simplifed structure and low polarization mode dispersion,” U.S. Patent 6,285,499, Sept. 4, 2001.
44. ——, “Optical circulators using beam angle tuners,” U.S. Patent 6,175,448, Jan. 16, 2001.